A Conceptual Modeling Study on Biosphere–Atmosphere Interactions and Its Implications for Physically Based Climate Modeling

GUILING WANG

Department of Civil and Environmental Engineering, University of Connecticut, Storrs, Connecticut

(Manuscript received 7 August 2003, in final form 23 November 2003)

ABSTRACT

This paper presents a conceptual modeling study on the behaviors of terrestrial biosphere–atmosphere systems as they relate to multiple equilibrium states and climate variability, and emphasizes their implications for physically based climate modeling. The conceptual biosphere–atmosphere model consists of equilibrium responses of vegetation and precipitation to each other, dynamics of the vegetation system, and stochastic forcing of precipitation representing the impact of atmospheric internal variability. Using precipitation as the atmospheric variable in describing the biosphere–atmosphere interactions, this model pertains to regions where vegetation growth is limited by water. Low moisture convergence in the atmosphere combined with high sensitivity of the atmospheric climate to vegetation changes provides the most favorable condition for the existence of multiple equilibrium states. In a coupled biosphere–atmosphere system with multiple equilibria, experiments varying the stochastic forcing indicate that atmospheric internal variability is an important factor in the long-term variability of the model climate and in its sensitivity to initial conditions. Specifically, the enhancement of low-frequency rainfall variability by vegetation dynamics is most pronounced with a moderate magnitude of atmospheric internal variability and is less pronounced if internal variability is either too large or too small; detecting the existence of multiple equilibria by examining the sensitivity of the coupled model climate to initial conditions is not always reliable since too large an internal variability reduces or even eliminates the model sensitivity to initial conditions. Findings from the conceptual model are confirmed using results from a physically based, synchronously coupled biosphere–atmosphere model. This study provides guidance for interpreting and understanding the model dependence of biosphere–atmosphere interaction studies using complex climate system models.

1. Introduction

The self-stablization of subtropical deserts through an albedo-dominated biogeophysical feedback as proposed by Charney (1975) raised the possibility that biosphere–atmosphere interactions may give rise to the existence of multiple equilibria in the earth's climate system. Specifically, the increase of albedo due to natural or manmade desertification causes a radiative cooling at the land surface that induces subsidence of the air, thus suppressing precipitation. This reduction of precipitation may cause further vegetation degradation and enhance the original desertification, leading the regional climate to evolve into a desertlike condition. While it has long been suggested that the earth's ice coverage can sustain different stable states under the same external forcing (e.g., Held and Suarez 1974), multiple equilibrium states that owe their existence to vegetation feedback represent a relatively new concept, and their implications for global climate modeling and prediction are not yet well understood. Using a simple conceptual model, this paper seeks to understand the behavior of the coupled biosphere–atmosphere system as it relates to vegetation feedback, multiple climate equilibria, and climate variability.

Over the past several decades, significant research effort has focused on studying the climatic impact of land use and land cover changes (e.g., Charney et al. 1977; Sud and Molod 1988; Dickinson and Henderson-Sellers 1988; Xue 1997; Hahmann and Dickinson 1997; Chase et al. 2001; Clark et al. 2001; Gates and Ließ 2001; Taylor et al. 2002; Pielke et al. 2002). This led to an improved understanding of the land surface feedback mechanism that involves not only changes in the energy budget due to vegetation-related albedo modification (as in the traditional Charney framework), but also changes in the hydrological cycle due to the vegetation control on evapotranspiration. At the same time, our capacity to predict the response of vegetation to changes in the environment has also been improved, thanks to the development of various biosphere models, including the earlier equilibrium vegetation models (e.g., Prentice et al. 1992) and the more recent dynamic global vegetation models (e.g., Foley et al. 1996; Brovkin et al. 1997; Cox et al. 2000; Sitch et al. 2003; Bonan

Corresponding author address: Dr. Guiling Wang, Department of Civil and Environmental Engineering, University of Connecticut, 261 Glenbrook Road, Storrs, CT 06269-2037.
E-mail: gwang@engr.uconn.edu

et al. 2003). Advances in these two directions together made it possible to represent the synchronously coupled biosphere–atmosphere system using complex numerical models that simulate not only the response of the atmosphere to vegetation changes but also the response of vegetation to changes in the atmosphere. This allowed us to test the hypothesis of multiple biosphere–atmosphere equilibria and to further scrutinize the role of dynamic vegetation in the earth's climate system using coupled biosphere–atmosphere models.

Multiple climate equilibria arising from biosphere–atmosphere interactions have been found in models of different complexity. Using a biome model iteratively coupled with the AGCM ECHAM, Claussen (1998) showed that the regional climate in West Africa and Saudi Arabia can develop into either of two different equilibria depending on the initial vegetation condition. Brovkin et al. (1998) developed a conceptual model for the atmosphere–vegetation system and showed that their conceptual model can explain the existence of multiple equilibrium states in ECHAM–BIOME. Wang and Eltahir (2000b), using a zonally symmetric atmospheric model synchronously coupled with the dynamic biosphere model Integrated Biosphere Simulator (IBIS; Foley et al. 1996) and considering the role of transient vegetation changes, illustrated the sensitivity of the coupled biosphere–atmosphere system in West Africa to initial vegetation conditions and further demonstrated that perturbations (natural or man-made) can cause reversible transitions of the regional climate system from a wet/green equilibrium to a dry/barren equilibrium or vice versa. The finding of multiple biosphere–atmosphere equilibria in climate models of different nature and of different complexity suggests, although does not confirm, that this special feature of the climate system is robust.

The multiple equilibrium behavior of the coupled biosphere–atmosphere system has significant implications for climate variability and changes. Wang and Eltahir (2000c,d, 2002) documented that the existence of multiple equilibrium states in their coupled model plays an important role in the decadal variability of the West African climate and in the response of this regional climate system to land use/land cover changes as well as CO_2 concentration changes. With increasingly common use of dynamic vegetation models in climate studies (e.g., Cox et al. 2000; Levis et al. 2000; Delire et al. 2003), it becomes essential that we understand the issue of multiple equilibria and its implications. Specifically, in order to accurately interpret the sensitivity of a model climate to external forcing, whether multiple equilibrium states exist, and, if they do, how their existence impacts the climate variability in that specific model should be documented and understood first.

The existence of multiple climate equilibria, or the lack of it, depends on the mutual sensitivity between the biosphere and the overlying atmosphere. As a result, multiple climate equilibria may exist in certain regions only depending on the regional atmospheric circulation patterns and vegetation surviving conditions. Similarly, for any specific region, some climate models may predict multiple equilibria, while others may not, depending on the differences in their ability to reproduce the most relevant responses and feedback processes. For complex climate system models, it is practically very difficult and computationally very expensive to diagnose whether multiple equilibrium states exist and to identify them where they do exist. This study aims to develop a theoretical understanding of biosphere–atmosphere interactions that can help delineate the multiple-equilibrium space of physically based biosphere–atmosphere models and to provide useful insight on the variability and sensitivity of the model climate. In section 2, a conceptual model of the coupled biosphere–atmosphere system is developed, emphasizing the dynamical nature of the system; section 3 describes the equilibrium solutions of the conceptual system; section 4 focuses on the long-term climate variability of this coupled system and its sensitivity to initial vegetation conditions as well as to atmospheric internal variability; section 5 provides a qualitative validation of the conceptual model using results from a physically based, coupled biosphere–atmosphere model; and conclusions are presented in section 6.

2. A conceptual model for the terrestrial biosphere–atmosphere system

Climate of the terrestrial biosphere–atmosphere system is governed by interactions between vegetation and the overlying atmosphere, of which precipitation–vegetation feedback is an important aspect. Over a major portion of the globe, vegetation growth is water-dependent, and changes of land cover (i.e., vegetation) can modify atmospheric processes thus resulting in changes of precipitation. Feedback between precipitation and vegetation takes place through various thermal, hydrological, and biogeochemical processes, and involves many key variables such as surface albedo and soil moisture. Instead of analyzing each aspect of the feedback in detail, this study focuses on two representative grand variables: annual precipitation amount P as a state variable of the atmosphere and vegetation amount V as a state variable of the biosphere. Here, vegetation amount V can be measured by leaf area index or green biomass.

In climate system models, and in the real world as well, vegetation and precipitation are often not in equilibrium with each other. Varying at time scales from years to centuries, vegetation is almost constantly in a transient state since a vegetation state in equilibrium with a given amount of precipitation cannot be reached unless the same level of precipitation persists sufficiently long in the climate sense. On the other hand, due to the large internal variability of the atmosphere, precipitation varies significantly from year to year even if vegetation condition were to stay the same. Here a con-

ceptual model of vegetation–precipitation feedback is developed that considers not only the equilibrium response of vegetation and precipitation to each other but also the dynamic nature of vegetation and the stochastic nature of precipitation.

Let V^* be the equilibrium vegetation, a virtual vegetation state in equilibrium with precipitation P so that $V^* = V^*(P)$, and let τ be the characteristic time scale of vegetation changes. If one assumes that the rate of changes in vegetation depends on the difference between its actual state and the equilibrium, vegetation can then be treated as a first-order dynamic system and its dynamics can be described by the following differential equation:

$$dV/dt = (V^* - V)/\tau, \tag{1}$$

where t is time. Use of Eq. (1) to model vegetation dynamics is not new to this study. In fact, it represents the general approach in modeling vegetation carbon dynamics (e.g., Gutman 1986; Foley et al. 1994; Brovkin et al. 1998; Dickinson et al. 1998; Zeng et al. 1999). Since V^* depends on the time-variant quantity P, Eq. (1) describes the tendency that water-limited vegetation in the real world grows denser as extra water from precipitation becomes available. Assuming that precipitation is the controlling factor for vegetation dynamics, this model pertains to regions where growth is limited by water as opposed to temperature or nonclimate factors.

Precipitation in this study is divided into two parts: a deterministic component P^* that depends on the atmosphere's boundary conditions including vegetation [i.e., $P^* = P^*(V)$] and a stochastic component $P'(t)$ that results from atmospheric internal variability. Assuming that $P'(t)$ follows the Gaussian distribution, precipitation P can be expressed as

$$P = P^* + \sigma R(t), \tag{2}$$

where t is time, σ is the standard deviation of precipitation attributable to atmospheric internal variability, and $R(t)$ is a random series that follows a standard normal distribution.

The dependence $V^*(P)$ that describes the equilibrium response of vegetation to precipitation changes can take various forms (e.g., hyperbolic, logistic, stepwise linear). In general, as precipitation goes from zero (or a minimum) to infinity (or a maximum), the sensitivity of vegetation increases before it decreases. For a given specific region, there exists a certain threshold value below which precipitation cannot support the growth of any vegetation. Therefore increasing the precipitation amount within a certain range from zero may not be able to cause much positive response of the vegetation. In the other extreme, under very wet conditions, an additional amount of water no longer enhances vegetation growth as the water demand of the biosphere is close to being saturated. The highest sensitivity is expected in between these two extremes. The functionality of $V^*(P)$ should be consistent with this general notion, but its specific form does not cause any qualitative difference in the results of this study. Brovkin et al. (1998) used a hyperbolic curve to fit the numerical experiments output from the coupled ECHAM–BIOME model. Here we also use a hyperbolic model for the simplicity of its parameterization:

$$V^*(P) = \begin{cases} 0 & (P < P_t) \\ V_{\max}[r/(1 + r)] & (P \geq P_t), \end{cases} \tag{3}$$

where $r = \max[0.0, (P - P_t)^3/(P_m - P_t)^3]$, P_t is the threshold precipitation amount below which no vegetation can survive, P_m the precipitation amount corresponding to the peak V^* sensitivity, and $V_{\max}$ the maximum amount of vegetation that can possibly exist if water is not limiting. The parameters P_t, P_m, and $V_{\max}$ depend on vegetation type as well as environmental conditions such as soil texture and nutrient availability.

The dependency $P^*(V)$ may also take various forms, and the validity of the theoretical analysis in this study does not depend on a specific form. Here we take its simplest form, the linear model:

$$P^*(V) = P_d + \alpha V, \tag{4}$$

where P_d (always nonnegative) is the amount of precipitation that would occur if no vegetation existed over the region of interest; α indicates the sensitivity of P^* to V. Guided by the numerous modeling studies (e.g., Xue 1997; Dickinson and Henderson-Sellers 1998) on the climatic impact of desertification and deforestation, we assume that precipitation increases with vegetation. The parameter α is therefore nonnegative. Obviously, both P_d and α depend on regional atmospheric circulation patterns.

Equations (1)–(4) together form a conceptual model of the terrestrial biosphere–atmosphere interactions. It treats the high-dimensional nonlinear chaotic climate system as a low-dimensional stochastically forced dynamic system, which is an approach commonly used in stochastic climate modeling (e.g., Demaree and Nicolis 1990; Penland and Matrosova 1994; Penland et al. 2000; Winkler et al. 2001). In this dynamically evolving conceptual system, V^* and P^* vary with time since they respectively depend on the time-variant precipitation (P) and vegetation (V). Note that Eqs. (3) and (4) represent one of many possible functionality forms of $V^*(P)$ and $P^*(V)$. For each specific form of functionality, its parameterization [e.g., values of P_t, P_m, P_d, and α if the functionality form in Eq. (3) and (4) are used] do influence the solution(s) or even the number of solutions of the conceptual system, as will be demonstrated later in section 3. However, the overall behavior of the system (e.g., the possible existence of multiple solutions, the system response to stochastic forcing and to initial conditions) does not depend on the specific functionality forms that $P^*(V)$ and $V^*(P)$ take.

In the following we will analyze the behavior of the

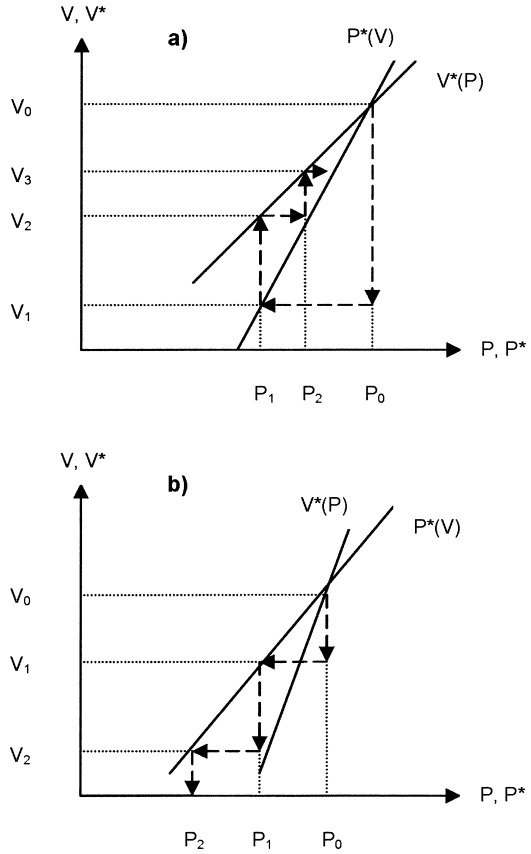

FIG. 1. Response to small perturbations of a water-limited biosphere–atmosphere system at (a) stable equilibrium and (b) unstable equilibrium.

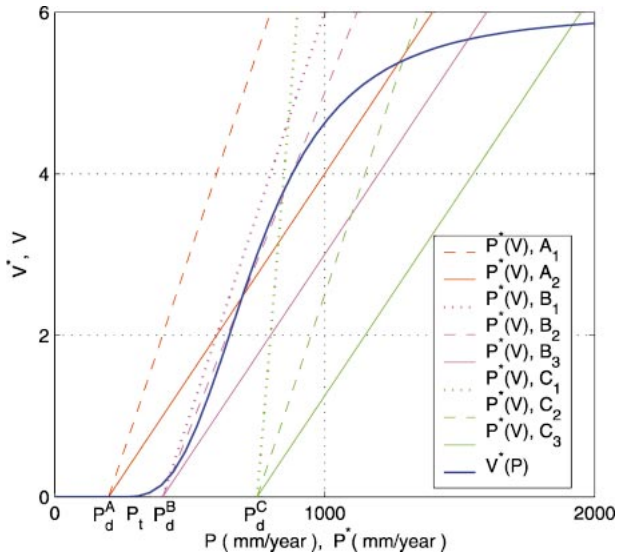

FIG. 2. Example diagrams for the equilibrium response of vegetation to precipitation changes $V^*(P)$ and of precipitation to vegetation changes $P^*(V)$.

simple conceptual model and how various factors and model parameters impact such behavior. In doing so, we emphasize the implications regarding complex physically based climate models.

3. Equilibrium solution(s) of the conceptual system

In the proposed conceptual model, the points of intersection between curves $V^*(P)$ and $P^*(V)$ define the equilibrium solutions of the dynamic system. However, some of these equilibrium solutions may not be stable, depending on the relative magnitude of dV^*/dP and $1/(dP^*/dV)$ at the point of intersection. If dV^*/dP is smaller, as illustrated in Fig. 1a, when a small disturbance causes vegetation (V) to decrease from V_0 to V_1, precipitation will respond and decreases from P_0 towards P_1, which is enough to support vegetation of amount V_2. Note that under this condition, V_2 is always larger than V_1. As a result, the system tends to bounce back and the equilibrium state is stable to the small perturbation. On the other hand, if dV^*/dP is larger than $1/(dP^*/dV)$, as illustrated in Fig. 1b, a small disturbance will trigger a positive feedback that leads the system away from the equilibrium state (V_0, P_0) to a neighboring stable equilibrium. This equilibrium is therefore not viable when interannual variability or disturbances of various forms are present and is labeled as unstable.

For a same $V^*(P)$ dependence, Fig. 2 demonstrates qualitatively how the number and characteristics of the equilibrium solution(s) of the conceptual system change as the parameterization of the $P^*(V)$ functionality in Eq. (4) varies. Note that the different $P^*(V)$ curves correspond to different regional atmospheric characteristics. Curve groups A, B, and C are distinguished by having the same amount of annual precipitation in the bare soil limit (i.e., P_d), with A having very little, B little, and C a moderate to large amount. Consequently, atmospheric moisture convergence increases from groups A to C since bare soil evaporation is generally small. Within each group, from curve types 1 to 3 (e.g., A_1 to A_2, B_1 to B_3, C_1 to C_3), precipitation becomes increasingly sensitive to changes at the land surface, that is, α in Eq. (4) increases. As far as the existence of multiple climate equilibria is concerned, there are several different types of atmospheric regimes based on Fig. 2: small bare land precipitation (P_d) combined with low sensitivity to land cover changes (α) gives rise to a regional system that has one arid stable equilibrium (e.g., A_1, B_1); small P_d combined with medium-to-high α defines a system that has two stable equilibrium states, a dry one and a wet one separated by an unstable medium equilibrium (e.g., A_2, B_2); except in regions with extremely small P_d, high α often leads to one stable wet equilibrium (e.g., B_3, C_3); finally, if P_d is sufficiently large, the system will always possess one stable wet equilibrium regardless of the magnitude of α (e.g., $C_1 - C_3$). Note that the above description of P_d as ''small'' or ''large'' is relative to the value of P_t in $V^*(P)$ [Eq. (3)], with small referring to ''not much larger than P_t.'' Similarly, the description

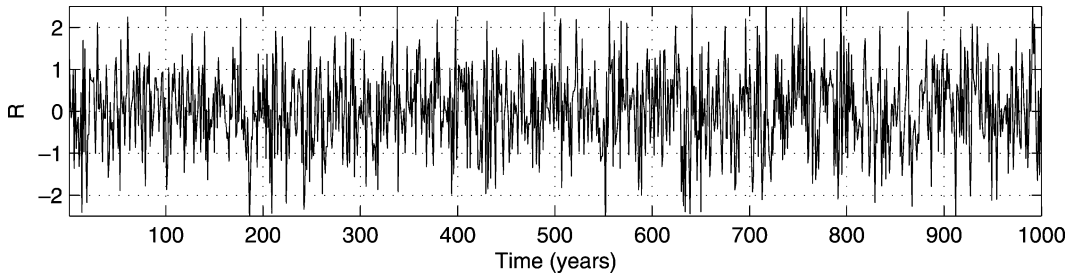

FIG. 3. A random time series of 1000 years that follows $N(0, 1)$ distribution, an example of $R(t)$ in Eq. (2).

of α as ''low,'' ''medium,'' or ''high'' is with respect to $1/(V^*/P)$.

For any given physically based climate system model, one can derive a corresponding parameterization for the $V^*(P)$ and $P^*(V)$ dependence by carrying out a manageable number of well-defined numerical experiments and fitting the experimental output. Driven with a set of different precipitation forcing, the terrestrial biosphere dynamics component of a climate system model can be run to define the $V^*(P)$ dependence; driven with a different prescription of vegetation conditions for the land surface, the atmospheric component of a climate system model can be run to define the $P^*(V)$ dependency. Note that these sensitivity experiments only need stand-alone simulations (as opposed to fully coupled simulations) that either prescribe the atmospheric forcing or prescribe vegetation conditions and are therefore computationally feasible. Fitting the output from these numerical sensitivity experiments leads to a parameterization for the vegetation–precipitation equilibrium response, which can then be used as a guide to whether a specific climate system model is predisposed to possess multiple equilibrium states in a certain region. Since simulated climate (including both the biosphere and the atmosphere components) and its sensitivity are often model dependent, one model may predict a single biosphere–atmosphere equilibrium while another predicts two equilibrium states coexisting. Similarly, as climate sensitivity and vegetation growth curves vary from region to region, so does the number of biosphere–atmosphere equilibria.

Although this study focuses on a natural biosphere–atmosphere system, it is worth pointing out that the number of equilibrium states of a regional climate system may change as a result of human activities. For example, in case of desertification, the loss of soil productivity due to erosion and nutrient leaching may be significant enough to cause an increase of P_t in Eq. (3). As a result, the $V^*(P)$ curve in Fig. 2 will shift toward the right-hand side, causing the equilibrium solution(s) of the coupled system to change towards greater aridity. Not only could the amount of equilibrium precipitation but also the number of solutions change in response to soil degradation. If the original system possessed one single wet equilibrium, the new system with degraded soil may have two (one wet and one dry) stable equilibrium solutions; similarly, if the original system featured two alternative equilibria, the degraded system may only allow for one dry equilibrium. In either case, the system becomes prone to drought occurrence.

4. Temporal variability of the conceptual system

The equilibrium solution(s) of the conceptual biosphere–atmosphere system as described above are dynamical ones. In reality the coupled system constantly oscillates around its equilibrium state(s) due to the internal variability of the atmosphere and the various external perturbations to which vegetation is subject (e.g., deforestation). In most physically based climate modeling, and in this study as well, it is assumed that vegetation growth is primarily influenced by atmosphere and land surface conditions, and the impact of other factors including external perturbations is not considered. Therefore, the atmospheric internal variability becomes the primary driving forcing for the temporal variation of the coupled biosphere–atmosphere system in the conceptual model. It also provides the forcing that drives the system away from its equilibria, while the biosphere–atmosphere feedback works to keep the system around its equilibrium. In the following we will demonstrate how atmospheric internal variability impacts the temporal behavior of the coupled system in the conceptual model. This will be done in combination with the model sensitivity to initial vegetation conditions, an important characteristic of systems with multiple equilibrium states.

First, let us take as an example the conceptual model parameterized as follows: $P_m = 750$ mm yr^{-1}, $P_t = 250$ mm yr^{-1}, $P_d = 400$ mm yr^{-1}, $\alpha = 120$ mm yr^{-1}. We can use leaf area index (LAI) to represent the vegetation amount and assume that $V_{\max}$ corresponds to a LAI of 6. This model has two stable equilibrium solutions: a relatively dry equilibrium with an annual precipitation of 434 mm yr^{-1} and a LAI of 0.29 (corresponding to 4.8% of $V_{\max}$); a relatively wet equilibrium with an annual precipitation of 880 mm yr^{-1} and a LAI of 4.0 (corresponding to 66.7% of $V_{\max}$). A random time series of 1000 years [$R(t)$ in Eq. (2)], as shown in Fig. 3, is used to drive the coupled biosphere–atmosphere system in the conceptual model, and vegetation is assumed to have a characteristic time scale [i.e., τ in Eq. (1)] of

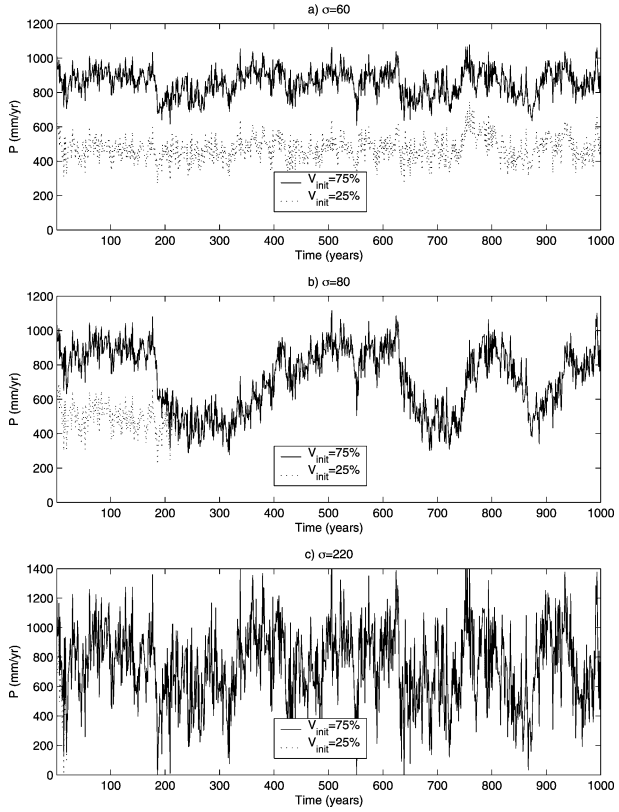

FIG. 4. Precipitation time series simulated by an example conceptual model driven by the random time series $R(t)$ shown in Fig. 3, with the precipitation standard deviation induced by atmospheric internal variability [σ in Eq. (2)] changing from (a) 60 to (b) 80 to (c) 220. Within each panel, different lines represent simulations with different initial vegetation condition V_{init}, where V_{init} stands for the vegetation amount in percentage of $V_{\max}$. This example conceptual model has two stable equilibrium solutions, and its parameterization is as follows: $P_m = 750$ mm yr^{-1}, $P_t = 250$ mm yr^{-1}, $P_d = 400$ mm yr^{-1}, $\alpha = 120$ mm yr^{-1}, and $V_{\max}$ corresponds to a LAI of 6.

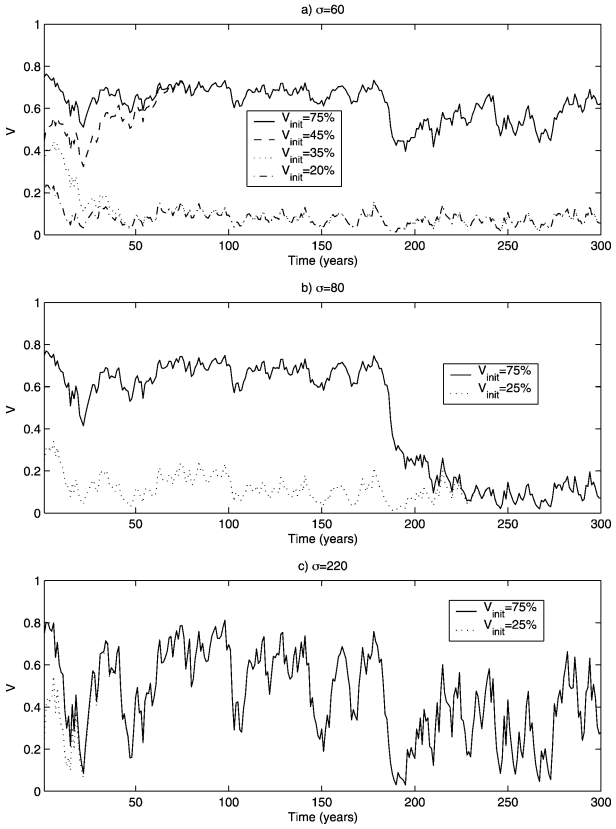

FIG. 5. As in Fig. 4 but for vegetation as a fraction of $V_{\max}$ and for the first three centuries of the conceptual model simulation.

2 yr. Figures 4 and 5 plot, respectively, the precipitation (in mm yr^{-1}) and vegetation (in fraction of $V_{\max}$) time series simulated by the conceptual model with a different magnitude of atmospheric internal variability: the value of σ in Eq. (2) (i.e., precipitation standard deviation attributable to the atmospheric internal variability) increases from top to bottom. Within each panel, different lines stand for experiments with different initial vegetation conditions. While Fig. 4 presents results for the whole millennium, Fig. 5 plots the first three centuries only to allow for a better view of details. According to these results, as the internal variability of the atmosphere (measured by σ) increases, the behavior of the simulated biosphere–atmosphere system varies significantly. Qualitatively, there are three different types of temporal variation of the system, as detailed in the following.

When σ is small compared to the precipitation difference between the two equilibrium states, the model climate is highly sensitive to initial conditions (Figs. 4a and 5a). Depending on its initial vegetation condition, the coupled system develops into one of two distinct climate regimes, each featuring oscillations around one of the system's two stable equilibrium solutions. The existence of these two distinct regimes causes uncertainty in validation and intercomparison of climate models since observation and different model simulations may describe different climate regimes. Without realizing the existence of multiple equilibrium states, one may attribute the difference between different equilibrium states to model deficiency or model differences.

As the value of σ gets larger (in Figs. 4b and 5b), the model's sensitivity to initial conditions decreases. Instead of remaining within one climate regime, the system switches between the two regimes aperiodically. It oscillates around one equilibrium state for quite a long time and then shifts to oscillations around another equilibrium state. The transition of the coupled system from one regime to another takes place rather abruptly. These aperiodic shifts of the system between two regimes result in significant climate fluctuations at decadal to centennial time scales. The impact of initial conditions lasts for as long as it takes for random atmospheric anomalies due to internal variability (or other forcings when considered) to trigger the system's first transition toward the alternative equilibrium. Therefore one may draw a

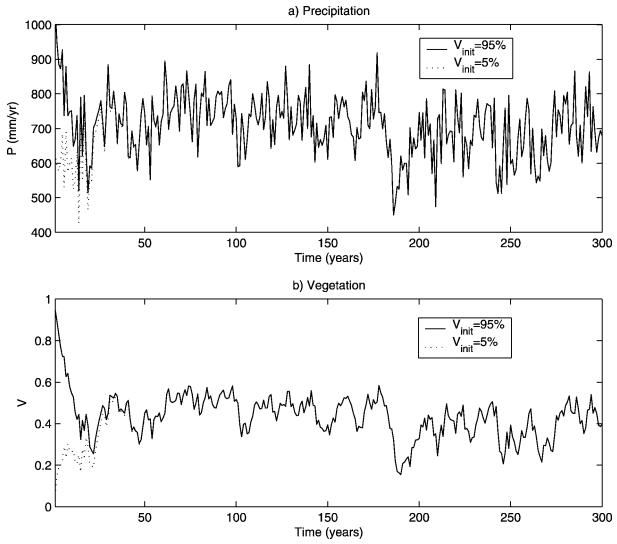

FIG. 6. (a) Precipitation and (b) vegetation as a fraction of V_{max}, simulated by a conceptual model that has only one equilibrium solution. Different lines within each panel represent results from simulations with different model initialization V_{init}. The model is driven by the random time series $R(t)$ in Fig. 3, and its parameterization is otherwise the same as the one in Fig. 4, except that $P_d = 500$ mm yr^{-1} and $\alpha = 80$ mm yr^{-1}.

completely different conclusion regarding the model sensitivity to initial conditions depending on the length of the simulation on which the conclusion is based.

Finally, when σ becomes sufficiently large (as in Figs. 4c and 5c), the model sensitivity to initial conditions almost disappears. The impact of initial conditions is quickly wiped out by random climate anomalies associated with the atmospheric internal variability. This large random forcing triggers frequent transitions of the coupled biosphere–atmosphere system between its two regimes/equilibria, and a new transition is often initiated before the previous transition is complete. As a result, the temporal variation of both precipitation and vegetation demonstrate more high-frequency fluctuations of very large amplitude, compared to Figs. 4b and 5b.

When a coupled system has only one equilibrium solution, its temporal variation resembles that of a system that has multiple equilibria but remains around one of them due to the smallness of the internal variability. For example, Fig. 6 shows the precipitation and vegetation time series of a conceptual model that is otherwise the same as the one shown in Figs. 4 and 5 except for its $P^*(V)$ parameterization. Here $P_d = 500$ mm yr^{-1} and $\alpha = 80$ mm yr^{-1}. This system has one equilibrium solution with an annual rainfall of 710 mm and a LAI of 2.6. Regardless of what the system starts with, as shown in Fig. 6, it always evolves into the same climate regime that features frequent oscillations around the system's equilibrium solution. Changes in the magnitude of σ do not cause any qualitative differences.

Compared with the white noise driving forcing in Fig. 3, the output of the conceptual system is significantly reddened for all types of parameterizations examined. This is clear from Fig. 7, which compares the spectra of the various precipitation time series presented above with the spectrum of the random driven forcing. Note that, if vegetation dynamics is ignored, that is, if τ in Eq. (1) approaches infinity, the temporal variation of the conceptual system will be completely captured by the stochastic term in Eq. (2), which is a white noise. Therefore, the spectrum comparison between the modeled precipitation time series and the random driven forcing reflects the impact of vegetation dynamics on the variability of the conceptual climate system. Under all parameterizations examined in this study, the model climate has more power at low frequency and less power at high frequency than the random climate anomalies, indicating that vegetation dynamics enhances the low-frequency variability of the coupled biosphere–atmosphere system and suppresses the high-frequency variability. This is in general consistency with the findings of physically based climate modeling studies (Wang and Eltahir 2000c; Zeng et al. 1999).

The degree to which vegetation dynamics enhances low-frequency climate variability is greatest for a biosphere–atmosphere system that alternates between two different regimes with a long residence time in each regime. The aperiodic transitions of the climate system between two alternative regimes result in a special form of low-frequency variability that add to the power of the climate at a very long time scale. Not surprisingly, as evident from Fig. 7, the precipitation time series of Fig. 4b features significantly more power at the centennial time scale than other precipitation time series. Instead of referring to the transition-induced low-frequency variability as ''red noise,'' we propose to call it the *Lorenz noise* to distinguish it from the reddening by vegetation dynamics unrelated to climate transitions and to reflect its similarity to switches of a Lorenz system between different basins of attraction (Lorenz 1963). The presence of Lorenz noise in physically based climate models requires special attention. Specifically, a transition of the system toward an alternative equilibrium, which would be part of the natural variability of the climate system under study, may be mistaken as a change of the climate, especially if it coincides with a climate-change forcing applied to the model. On the other hand, the response of the modeled climate system to climate-change forcing will be extremely nonlinear. When the system state is close to the boundary between the attraction basins of the two equilibria, a very small forcing may cause the system to cross the threshold and settle into a different equilibrium state within a very short time, resulting in an abrupt climate shift.

In physically based modeling studies of biosphere–atmosphere interactions, as far as the topic of multiple equilibria is concerned, one of the most important questions to address is whether the existence of multiple equilibrium states can be detected from the model-simulated time series of climate state variables. Generally,

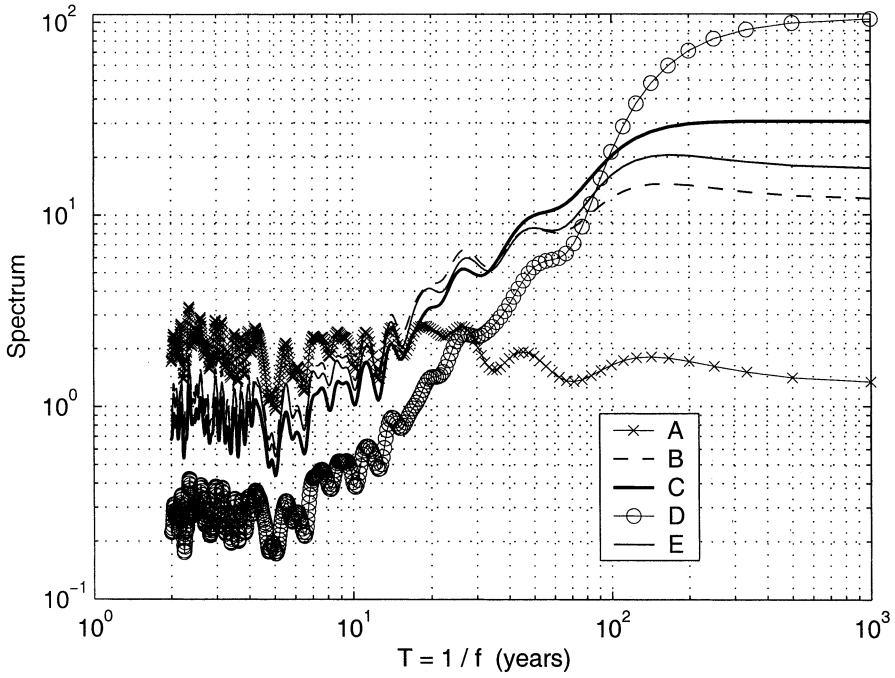

FIG. 7. The spectrum of different simulated precipitation time series (B, C, D, and E) compared with the spectrum of the model driving forcing (A). Here, B stands for the precipitation time series in Fig. 6a with $V_{init} = 90\%$; C stands for the precipitation time series in Fig. 4a with $V_{init} = 75\%$; D stands for the time series in Fig. 4b with $V_{init} = 75\%$; and *E* stands for the time series in Fig. 4c with $V_{init} = 75\%$. The model driving forcing refers to the random time series in Fig. 3.

when multiple equilibria do exist, the model climate is expected to show sensitivity to initial conditions. A reasonable methodology is therefore to compare the output of two long climate simulations that have extremely different initial vegetation states: for example, one starting with a desert land surface and one starting with a forest-covered land surface (Claussen 1998; Wang and Eltahir 2000b). However, according to Figs. 4c and 5c, even when multiple equilibrium solutions do exist, a system's sensitivity to initial conditions may not be obvious from the model output if the internal variability is too large. Such a large internal variability can be a true characteristic of the regional climate or result from a model deficiency causing overestimation of the atmospheric internal variability. When it reflects the true climate characteristics, none of the existing multiple equilibrium states will be self-sustaining. However, when it is a model deficiency, one may draw a false conclusion regarding the existence of multiple climate equilibria based on the lack of sensitivity of the model output to initial conditions. As a result, the impact of multiple equilibrium on the variability and changes of the regional climate may be mistakenly ignored. Therefore, it is essential for climate models to reproduce not only the mean climate but also the climate variability.

5. Example from physically based modeling

The impact of atmospheric internal variability on the structure of the biosphere–atmosphere climate, as derived from the stochastically driven dynamic model depicted above, can be qualitatively validated using physically based models. In the following we use a zonally symmetric biosphere–atmosphere model (ZonalBAM: Wang and Eltahir 2000a) as an example. ZonalBAM was developed to study the regional climate system of West Africa. It includes a terrestrial biosphere model (IBIS by Foley et al. 1996) and a zonally symmetric atmospheric model. The model domain spans from pole to pole, with land located north of 5°N and ocean to the south. Over ocean, a prescribed sea surface temperature (SST) provides the lower boundary condition for the atmosphere; over land, terrestrial biosphere and the overlying atmosphere are synchronously coupled and therefore coevolve with each other.

Over the Sahel region of West Africa, the biosphere–atmosphere system simulated by ZonalBAM possesses two stable equilibrium states close to the present climate under the same SST forcing (Wang and Eltahir 2000b,c), one featuring a healthy grass ecosystem with abundant rain and the other is desertlike; between the two stable ones exists an unstable equilibrium that is not viable under the influence of disturbances in the form of SST interannual variability. The $P^*(V)$ and $V^*(P)$ curves derived from ZonalBAM using the methodology proposed in section 3 are plotted in Fig. 8, where the brackets mark the approximate locations of the points of intersection between the two curves. Based on Fig. 1, it is clear that the curves in Fig. 8 define two stable equi-

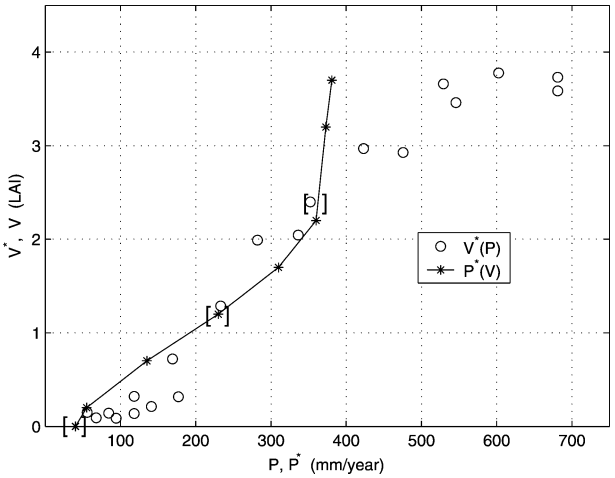

FIG. 8. The equilibrium response $P^*(V)$ and $V^*(P)$ as derived from the physically based biosphere–atmosphere model ZonalBAM, where the heavy brackets mark the approximate location of the equilibrium solutions of the coupled system. Note that the middle equilibrium is not stable.

librium solutions separated by an unstable equilibrium. This is consistent with the documented existence of multiple equilibrium states in ZonalBAM (Wang and Eltahir 2000b,c).

To derive the $V^*(P)$ relationship in Fig. 8, the biosphere model IBIS was run for 80 years in the stand-alone mode, driven with the daily climatological National Centers for Environmental Prediction–National Center for Atmospheric Research (NCEP–NCAR) reanalysis data (Kalnay et al. 1996) at $2^\circ \times 2^\circ$ resolution. The $V^*(P)$ scattering diagram in Fig. 8 is based on the simulated vegetation from grid points in the Sahel region at 17°N where the difference between the two stable equilibria of ZonalBAM is most pronounced. Note that IBIS in the stand-alone mode is not constrained by the zonal symmetry of the atmosphere as it is in the coupled model ZonalBAM. Therefore it can be run with any spatial resolution and configuration. For the $2^\circ \times 2^\circ$ simulation used here, multiple grid points exist at the same latitude, causing the scattering of the $V^*(P)$ relationship. To derive the $P^*(V)$ curve, a group of experiments were run using ZonalBAM with LAI in the grassland region of West Africa prescribed to different values. Different experiments are driven by the same climatological SST forcing, and have the same specified LAI at the grid points south of the Sahel where trees exist. The $P^*(V)$ curve in Fig. 8 presents the 5-yr average of annual precipitation versus LAI at the grid point closest to 17°N. Due to the zonal symmetry of the atmosphere model, only one grid point is plotted for each $P^*(V)$ experiments.

Vegetation in West Africa has a sharp gradient in the meridional direction, and numerical modeling studies (e.g., Zheng and Eltahir 1997) showed that vegetation changes in the region south of Sahel can have a considerable impact on precipitation over the Sahel. Therefore, $P^*(V)$ for the Sahel region may shift slightly when vegetation distribution south of the Sahel is specified differently. However, qualitatively, the extremely low precipitation under desert land condition and the high sensitivity of precipitation to LAI changes in ZonalBAM documented in Fig. 8 are highly favorable for multiple precipitation–vegetation equilibrium states to exist, according to Fig. 2. The actual existence of two stable equilibrium states in ZonalBAM (Wang and Eltahir 2000c) makes it an ideal tool to test the understanding derived from the conceptual model regarding climate variability of the coupled biosphere–atmosphere system.

Due to the lack of zonal disturbance in a zonally symmetric model, the atmospheric internal variability in ZonalBAM is minimal. However, for the biosphere–atmosphere system of West Africa in ZonalBAM, the atmospheric response to oceanic forcing acts similarly to the atmospheric internal variability. Therefore, the SST-induced atmospheric variability at the interannual time scale can be treated as the model internal variability if the focus is over land. Accordingly, one can change this pseudo-internal variability by modifying the SST forcing. Here the SST forcing is defined as the SST anomaly relative to a predefined climatology.

To demonstrate how the simulated regional biosphere–atmosphere climate responds to atmospheric internal variability, results from three pairs of experiments using ZonalBAM are presented here. Each pair includes one experiment initialized with dense grass in the Sahel region (labeled as Wet) and one initialized with 80% less grass (labeled as Dry). In the first pair, ZonalBAM was run for 100 years driven with observed SST forcing extracted from the Global Sea Ice and Sea Surface Temperature (GISST) dataset (Parker et al. 1985; Rayner et al. 1996) for the period 1898–1997 (Wet_1 and Dry_1); in the second pair, SST anomalies are artificially increased to 1.5 times of their actual value for the same time period (Wet_1.5 and Dry_1.5); in the third pair, two times of the actual SST anomalies are applied (Wet_2 and Dry_2). Here the artificially enhanced SST forcing is used to increase the pseudo-internal atmospheric variability in the model. Figures 9 and 10 plot the time series of annual precipitation and growing season grass LAI at the grid point near 17°N simulated in the six experiments described above.

Under the influence of ''internal'' atmospheric variability induced by the observed SST forcing, the coupled biosphere–atmosphere system of the Sahel can sustain two distinctive climate regimes, each resulting from oscillations around the respective equilibrium state (Figs. 9a and 10a). When such internal variability increases (as forced by the enhanced SST forcing), the biosphere–atmosphere interactions can no longer keep the coupled system within one climate regime. Instead, the system alternates between the two regimes and can reside in one regime for decades at a time, causing significant power at very low frequency in the climate

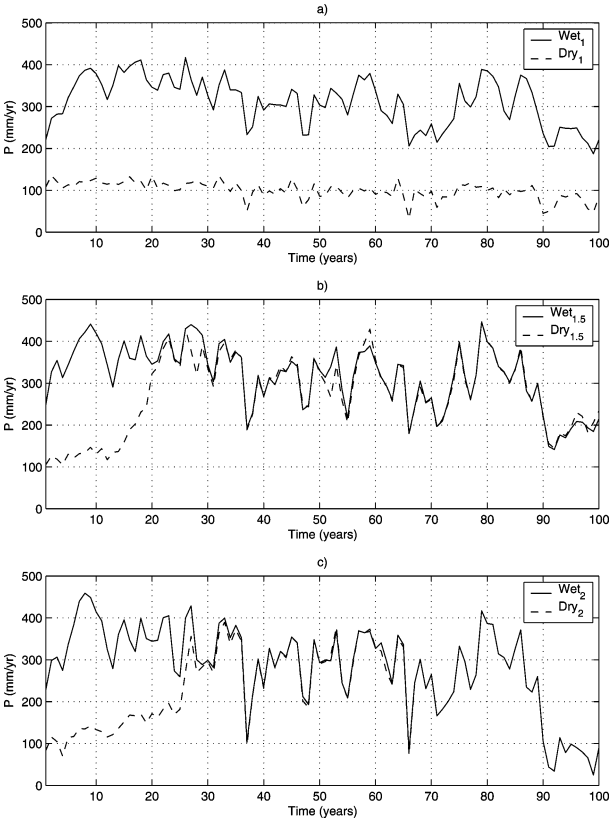

FIG. 9. Precipitation at about 17°N in the Sahel, simulated in different experiments using ZonalBAM driven with (a) the observed oceanic forcing during the 100 years from 1898 to 1997; (b) oceanic forcing equivalent to 1.5 times the observed; and (c) oceanic forcing equivalent to 2 times the observed. Differences between the corresponding Wet and Dry experiments are due to their different initial vegetation conditions with the initial LAI in the Dry experiments being 20% of that in the Wet experiments.

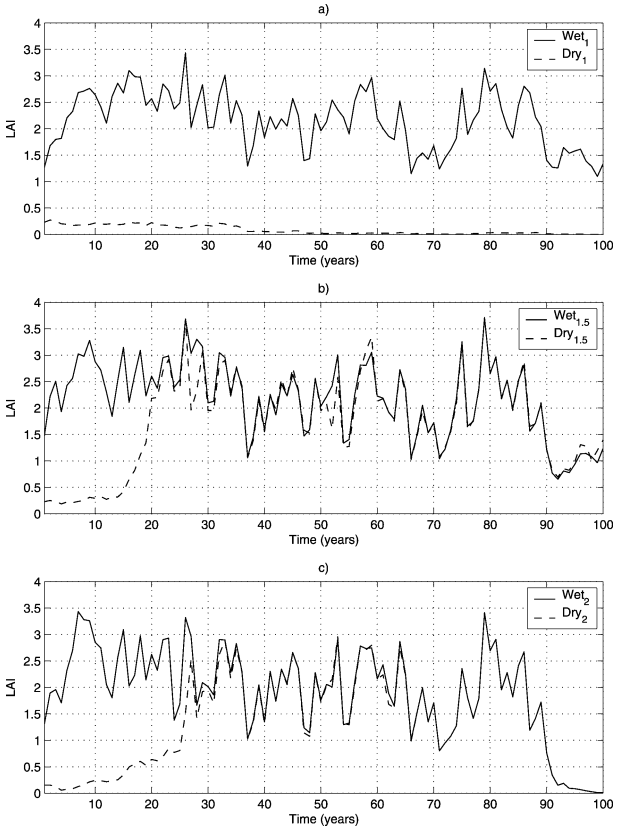

FIG. 10. As Fig. 8 but for the peak growing season LAI for grass.

variance. For example, in experiment Dry_1.5 (Figs. 9b and 10b), the system made a transition from dry/desert to wet/green regime right before year 20 of the simulation and persists in that regime for the rest of the simulation period. As the internal variability further increases, the residence time in each regime decreases, and the transitions between different regimes become more frequent. As shown in Figs. 9c and 10c, the Dry_2 experiment includes a dry-to-wet transition in the third decade and a wet-to-dry transition around year 90 of the simulation. In addition, in the fourth and seventh decades, a wet-to-dry transition was initiated, but only to be reversed before the transition was complete. Similar to the conceptual model analysis documented in section 4, the physically based numerical experiments presented here indicate that in systems that possess multiple equilibrium states, if the internal variability is large or overestimated, the model sensitivity to initial conditions disappears after the first climate transition.

The response of the climate structure to model internal variability in ZonalBAM is qualitatively the same as what the conceptual model indicates in section 4. Changes from top to bottom in Fig. 4 bears remarkable similarity to those in Fig. 9, suggesting that the conceptual model proposed in this study provides a useful tool for interpreting/predicting the behavior of the coupled biosphere–atmosphere system simulated by complex, physically based numerical models.

6. Conclusions

A stochastically driven, nonlinear dynamic model of terrestrial biosphere–atmosphere interactions is developed. The model is used to study the existence of multiple equilibrium states in coupled biosphere–atmosphere systems, long-term variability of the system, and its sensitivity to atmospheric internal variability and to vegetation initialization. Theoretical analyses based on this conceptual model appear to be supported by results from a zonally symmetric, physically based biosphere–atmosphere model. This study supports the following conclusions:

1) Generally speaking, biosphere–atmosphere interactions are able to give rise to multiple climate equilibrium states. Whether the climate system in a specific region is predisposed to have multiple equilibria depends on the regional atmospheric circulation pat-

tern and vegetation growing conditions. In regions where growth is limited by water, extremely low moisture convergence in the atmosphere and high sensitivity of precipitation to vegetation changes together provide the most favorable condition for multiple equilibrium states to coexist.

2) Whether a physically based climate model can capture the existence of multiple equilibrium states where they do exist depends on how the model reproduces the most relevant climate sensitivities. These include the response of atmospheric processes to vegetation changes and the response of vegetation to changes in the atmosphere. A set of experiments using the atmospheric model specifying different vegetation conditions and a set of experiments using the dynamic vegetation model driven with different atmospheric forcing can help diagnose the existence of multiple biosphere–atmosphere equilibria in the coupled model.
3) How the existence of multiple equilibrium states impacts climate variability in a model depends on the magnitude of atmospheric internal variability. When the internal variability is small, the climate system resides within either of two distinct, self-sustaining regimes depending on the initial conditions; large internal variability causes aperiodic transitions of the system between alternative regimes/equilibria, leading to climate fluctuations at decadal–centennial time scales. However, if the internal variability is overly large, climate transition will become so frequent and residence time in each regime so short that climate variability is dominated by rapid oscillation of very large amplitude.
4) Detecting the existence of multiple equilibria by examining the sensitivity of the coupled model to initial conditions is not always reliable, depending on the magnitude of atmospheric internal variability. When multiple equilibria do exist, an overly large internal variability in the atmospheric climate reduces or even eliminates the model sensitivity to initial conditions.
5) Compared with a climate system where the biosphere was assumed to be static, vegetation dynamics enhances the power of climate variance at low frequencies. The degree of such enhancement varies with the atmospheric internal variability. The maximum effect is expected where the climate system has multiple equilibrium states and the internal variability is able to trigger the system to shift between different equilibria with very long residence time at each of them. This does not occur if the internal variability is too small or too large compared with the distance between different equilibrium states.

Multiple equilibrium states arising from biosphere–atmosphere interactions can be true characteristics of the earth's climate system and can have significant implications for climate variability and climate changes. This study develops some theoretical understanding about why multiple equilibrium states exist where they do, what role they play in shaping the climate variability, and how the atmospheric internal variability impacts the behavior of a system with multiple equilibria. This will provide useful guidance for studying the issue of multiple equilibrium states and their impact using complex global climate system models.

One important assumption of the conceptual model used in this study is that precipitation is the primary control of vegetation. The theoretical understanding thus developed regarding the existence of multiple equilibrium states is most pertinent for regions where water availability is the limiting factor for vegetation growth, and for regions where human activities (e.g., deforestation and desertification) can potentially lead to future water stress in the environment although water is not limiting at the present. These regions are typically located in the Tropics and subtropics, and some in the middle latitudes. When applying the conceptual understanding developed here to a global climate system model, the derivation of the $P^*(V)$ and $V^*(P)$ curves should be carried out at the regional scale since the vegetation growth curve may vary significantly from region to region. In the high latitudes where temperature sets the limit for vegetation growth, the existence of multiple equilibrium states is also of great scientific interest (e.g., Levis et al. 1999; Brovkin et al. 2003), and a conceptual model for vegetation–temperature feedback can be developed in analogy to the model proposed in this study.

Acknowledgments. The author would like to thank Dr. Robert Dickinson at the Georgia Institute of Technology for his constructive comments on an earlier version of this paper. Comments and suggestions from Dr. Christine Delire at the University of Wisconsin and an anonymous reviewer are also gratefully acknowledged.

REFERENCES

Bonan, G. B., S. Levis, S. Sitch, M. Vertenstein, and K. W. Oleson, 2003: A dynamic global vegetation model for use with climate models: Concepts and description of simulated vegetation dynamics. *Global Change Biol.,* **9,** 1543–1566.

Brovkin, V., A. Ganopolski, and Y. Svirezhev, 1997: A continuous climate–vegetation classification for use in climate–biosphere studies. *Ecol. Model.,* **101,** 251–261.

——, M. Claussen, V. Petoukhov, and A. Ganopolski, 1998: On the stability of the atmosphere–vegetation system in the Sahara/Sahel region. *J. Geophys. Res.,* **103D,** 31 613–31 624.

——, S. Levis, M.-F. Loutre, M. Crucifix, M. Claussen, A. Ganopolski, C. Kubatzki, and V. Petoukhov, 2003: Stability analysis of the climate–vegetation system in the northern high latitudes. *Climatic Change,* **57,** 119–138.

Charney, J. G., 1975: Dynamics of deserts and drought in the Sahel. *Quart. J. Roy. Meteor. Soc.,* **101,** 193–202.

——, W. J. Quirk, S. Chow, and J. Kornfield, 1977: A comparative study of the effects of albedo change on drought in semi-arid regions. *J. Atmos. Sci.,* **34,** 1366–1385.

Chase, T. N., R. A. Pielke Sr., T. G. F. Kittel, M. Zhao, A. J. Pitman, S. W. Running, and R. R. Nemani, 2001: Relative climatic effects of land cover change and elevated carbon dioxide combined with

aerosols: A comparison of model results and observations. *J. Geophys. Res.,* **106,** 31 685–31 691.
Clark, D. B., Y.-K. Xue, R. J. Harding, and P. J. Valdes, 2001: Modeling the impact of land surface degradation on the climate of tropical North Africa. *J. Climate,* **14,** 1809–1822.
Claussen, M., 1998: On multiple solutions of the atmosphere–vegetation system in present-day climate. *Global Change Biol.,* **4,** 549–559.
Cox, P. M., R. A. Betts, C. D. Jones, S. A. Spall, and I. J. Totterdell, 2000: Acceleration of global warming due to carbon-cycle feedbacks in a coupled climate model. *Nature,* **408,** 184–187.
Delire, C., J. A. Foley, and S. Thompson, 2003: Evaluating the carbon cycle of a coupled atmosphere–biosphere model. *Global Biogeochem. Cycles,* **17,** 1012, doi:10.1029/2002GB001870.
Demaree, G. R., and C. Nicolis, 1990: Onset of Sahelian drought viewed as a fluctuation-induced transition. *Quart. J. Roy. Meteor. Soc.,* **116,** 221–238.
Dickinson, R. E., and A. Henderson-Sellers, 1988: Modeling tropical deforestation: A study of GCM land surface parameterization. *Quart. J. Roy. Meteor. Soc.,* **114,** 439–462.
——, M. Shaikh, R. Bryant, and L. Graumlich, 1998: Interactive canopies for a climate model. *J. Climate,* **11,** 2823–2836.
Foley, J. A., I. C. Prentice, N. Ramankutty, S. Levis, D. Pollard, S. Sitch, and A. F. Haxeltine, 1996: An integrated biosphere model of land surface processes, terrestrial carbon balance, and vegetation dynamics. *Global Biogeochem. Cycles,* **10,** 603–628.
Gates, L. D., and S. Ließ, 2001: Impacts of deforestation and desertification in the Mediterranean region as simulated by the MPI atmospheric GCM. *Global Planet. Change,* **30,** 309–328.
Gutman, G., 1986: On modeling dynamics of geobotanic state–climate interaction. *J. Atmos. Sci.,* **43,** 305–307.
Hahmann, A. N., and R. E. Dickinson, 1997: RCCM2-BATS model over tropical South America: Applications to tropical deforestation. *J. Climate,* **10,** 1944–1964.
Held, I. M., and M. J. Suarez, 1974: Simple albedo feedback models of the ice caps. *Tellus,* **26,** 613–628.
Kalnay, E., and Coauthors, 1996: The NCEP/NCAR 40-Year Reanalysis Project. *Bull. Amer. Meteor. Soc.,* **77,** 437–471.
Levis, S., J. A. Foley, V. Brovkin, and D. Pollard, 1999: On the stability of the high-latitude climate–vegetation system in a coupled atmosphere–biosphere model. *Global Ecol. Biogeogr.,* **8,** 489–500.
——, ——, and D. Pollard, 2000: Large-scale vegetation feedbacks on a doubled CO_2 climate. *J. Climate,* **13,** 1212–1325.
Lorenz, E. N., 1963: Deterministic nonperiodic flow. *J. Atmos. Sci.,* **20,** 130–141.
Parker, D. E., M. Jackson, and E. B. Horton, 1985: The GISST2.2 sea surface temperature and sea-ice climatology. Climate Research Tech. Note 63 (CRTN63), Met Office, Bracknell, Berkshire, United Kingdom, 35 pp.
Penland, C., and L. Matrosova, 1994: A balance condition for stochastic numerical models with application to the El Niño–Southern Oscillation. *J. Climate,* **7,** 1352–1372.
——, M. Flugel, and P. Chang, 2000: Identification of dynamical regimes in an intermediate coupled ocean–atmosphere model. *J. Climate,* **13,** 2105–2115.
Pielke, R. A., G. Marland, R. A. Betts, T. N. Chase, J. L. Eastman, J. C. Niles, D. S. Niyogi, and S. W. Running, 2002: The influence of land-use change and landscape dynamics on the climate system: Relevance to climate-change policy beyond the radiative effect of greenhouse gases. *Philos. Trans. Roy. Soc. London,* **360A,** 1705–1719.
Prentice, I. C., W. Cramer, S. P. Harrison, R. Leemans, R. A. Monserud, and A. M. Solomon, 1992: A global biome model based on plant physiology and dominance, soil properties, and climate. *J. Biogeogr.,* **19,** 117–134.
Rayner, N. A., E. B. Horton, D. E. Parker, C. K. Folland, and R. B. Hackett, 1996: Version 2.2 of the global sea-ice and sea surface temperature data set, 1903–1994. Climate Research Tech. Note 74 (CRTN 74), Met Office, Bracknell, Berkshire, United Kingdom, 21 pp.
Sitch, S., and Coauthors, 2003: Evaluation of ecosystem dynamics, plant geography and terrestrial carbon cycling in the LPJ dynamic global vegetation model. *Global Change Biol.,* **9,** 161–185.
Sud, Y. C., and A. Molod, 1988: A GCM simulation study of the influence of Saharan evapotranspiration and surface-albedo anomalies on July circulation and rainfall. *Mon. Wea. Rev.,* **116,** 2388–2400.
Taylor, C. M., E. F. Lambin, N. Stephenne, R. J. Harding, and R. L. Essery, 2002: The influence of land use change on climate in the Sahel. *J. Climate,* **15,** 3615–3629.
Wang, G. L., and E. A. B. Eltahir, 2000a: Biosphere–atmosphere interactions over West Africa. 1. Development and validation of a coupled dynamic model. *Quart. J. Roy. Meteor. Soc.,* **126,** 1239–1260.
——, and ——, 2000b: Biosphere–atmosphere interactions over West Africa. 2. Multiple climate equilibria. *Quart. J. Roy. Meteor. Soc.,* **126,** 1261–1280.
——, and ——, 2000c: Role of ecosystem dynamics in the low-frequency variability of the Sahel rainfall. *Water Resour. Res.,* **36,** 1013–1021.
——, and ——, 2000d: Ecosystem dynamics and the Sahel drought. *Geophys. Res. Lett.,* **27,** 795–798.
——, and ——, 2002: Response of the biosphere–atmosphere system in West Africa to CO_2 concentration changes. *Global Change Biol.,* **8,** 1169–1182.
Winkler, C. R., M. Newman, and P. D. Sardeshmukh, 2001: A linear model of wintertime low-frequency variability. Part I: Formulation and forecast skill. *J. Climate,* **14,** 4474–4494.
Xue, Y.-K., 1997: Biosphere feedback on regional climate in tropical North Africa. *Quart. J. Roy. Meteor. Soc.,* **123,** 1483–1515.
Zeng, N., J. D. Neelin, K. M. Lau, and C. J. Tucker, 1999: Enhancement of interdecadal climate variability in the Sahel by vegetation interaction. *Science,* **286,** 1537–1540.
Zheng, X. Y., and E. A. B. Eltahir, 1997: The response to deforestation and desertification in a model of West African monsoons. *Geophys. Res. Lett.,* **24,** 155–158.